CHEMICAL BATH DEPOSITION OF ZINC OXIDE NANOFLOWER FILM ON SILVER NANOPARTICLE SEED LAYER

Su Myat Aung[1], Myo Aung[2] and Nan Thidar Chit Swe[3]

Abstract

Zinc oxide nanoflower with hexagonal structure was achieved by using chemical bath deposition method under atmospheric pressure by using zinc nitrate hexahydrate [$Zn(NO_3)_2.6H_2O$] and hexamethylene-tetramine ($C_6H_{12}N_4$) at constant temperature 93ºC and the deposition time of 2 h. The prepared the film was grown on the suface of silver nanoparticles. The surface morphologies and the structural characterization of zinc oxide (ZnO) nanoflowers and silver nanoparticles were characterized by Scanning Electron Microscope (SEM) and X-ray Diffraction (XRD) technique. The SEM results revealed that the petal lengths of the zinc oxide (ZnO) nanoflowers were up to more than 2 nm in diameter from 200 nm to 300 nm. The XRD pattern of the sample revealed that ZnO nanoflowers have hexagonal crystallite structure.

Key words: Zinc Oxide nanoflowers, silver nanoparicles, seed layer

Introduction

Zinc oxide (ZnO) is a wide direct band gap (3.37eV) semiconductor which possesses high dielectric constant and excitation with high binding energy (60 MeV) at room temperature. The melting point of zinc oxide (ZnO) is 1954 ºC, this determines high thermal and chemical stability. It also shows piezoelectricity. It is nontoxic material which is cheaply available. ZnO is also biocompatible, biodegradable, and biosafe for medical and environmental applications (Xia *et al*, 2003). Due to these properties, ZnO is a material of huge technological importance. Due to their remarkable performance in electronics, optics, and photonics, ZnO nanostructures are attractive candidates for many applications such as UV lasers, light-emitting diodes, solar cells, nanogenerators, gas sensors, photodetectors (Cao *el al*, 2006).

Variety of nanostructures of ZnO can be grown by using different methods. In general, there are two distinct approaches to create

1. Demonstrator, Department of Physics, Loikaw University
2. Lecturer, Universities' Research Center, University of Yangon
3. Lecturer, Universities' Research Center, University of Yangon

nanostructures: top-down and bottom-up strategies. The top-down approach, etching and lithography in bulk materials is created to form functional devices. In the bottom-up approach, functional nanostructures are assembled from well-defined chemically and/or physically synthesized building blocks (Feng L *et al*, 2010).

There are various techniques to synthesize zinc oxide (ZnO) nanostructures such as metal organic chemical vapor deposition (MOCVD) (Park *et al*, 2002), molecular beam epitaxy (MBE), pulse laser deposition (PLD) and chemical vapor deposition (CVD). But these techniques are very expensive, highly toxic, high cost in environmental disposal and they need high vacuum equipment (Samanta P *et al*, 2009). Nonetheless, it is essential to find another technique to grow zinc oxide (ZnO) nanostructures that offers low cost and does not need high vacuum equipment. One of the most interesting method of ZnO synthesis is chemical bath deposition (CBD) (Yi S-H *et al*, 2007). (.It does not need complicated and expensive instruments and it allows for deposition of ZnO on different substrates. Nowadays, it is believed that chemical bath deposition (CBD) technique might be the cheapest method to deposit ZnO nanostructures. It does not require sophisticated instruments while the starting chemicals are commonly available and cheap, and the preparation parameters are easily controlled. And this technique does not need high vacuum equipment (Gowthaman P *et al*, 2011). In this paper, zinc oxide (ZnO) nanostructures such as nanoflowers and nanorods are synthesized by a bottom-up approach.

Experimental

2.1 Materials

Analytical grade (BDH, England) Zinc Nitrate Hexahydrate [$Zn(NO_3)_2.6H_2O$], Hexamethylenetetramine ($C_6H_{12}N_4$), Silver Nitrate ($AgNO_3$, 99.9%), Ethanol (EtOH) Polyvinylpyrroli done (PVP), Ethylene Glycol (EG) were used as starting precursor. All chemicals were used as purchased without further purification.

2.2 Cleaning Procedure of Glass Substrate

The very first step before the CBD proper is the washing of glass substrate in order to remove dirt and impurities that may have unknowingly settled on the glass substrate. This is done by washing in several substances, namely: acetone, distilled water, ethanol, distilled water again, hydrochloric acid (HCl) and lastly distilled water. These glass substrates are then dried in air blow at room temperature.

2.3 Synthesis of Silver nanoparticles (Ag NPs) and fabrication of Ag seeding layer

Silver nanoparticles were synthesized by reducing $AgNO_3$ as metal precursor salt in Ethylene Glycol (EG) which was used as not only reducing agent but also solvent and PVP as a capping agent. $AgNO_3$ solution (94 mM, in EG) and PVP solution (30K) (147 mM, in EG) were completely dissolved by using magnetic stirring at room temperature. First, 30 mL of EG in a flask was heated at 170 °C in a heating mantle with stirring rate 150 rpm for 30 minutes. Mixed PVP/ethylene glycol was added to prepared solution, followed by AgNO3 /ethylene glycol drop wise to the solution over dropping at a rate of 1ml min^{-1}. After adding all reagents, the mixture turned yellow indicating the appearance of Ag nanoparticle. (Nan *et al*, 2018). The reaction continue for 40 minutes until the reaction finished completely with formed slightly gray-white suspensions.

The product was diluted with acetone (1:5 by volume) and centrifuged at 10000 rpm for 20 min. The supernatant containing organic residues could be removed using a pipette. This centrifugation procedure could be repeated three times with ethanol. Purified Silver nanoparticles solution was mixed with 2-propanol (1:1v/v) and sonicated for 15 minutes to get homogenous ink solution for making seed layer. This solution was coated on glass substrates by rod coating method. After being placed in the air for few minutes at room temperature, the Ag nanoparticle layer was achieved as a solid and thin layer on the glass substrate.

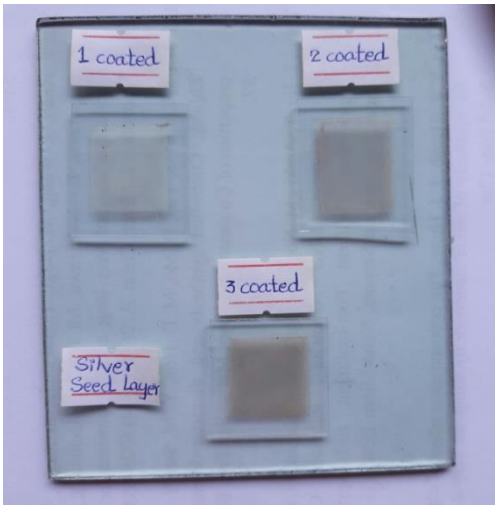

Figure 1: (a) Silver nanoparticle (b) Silver nanoparticles seed layer coated on glass slide

2.3 Chemical Bath Deposition (CBD) Method

For chemical bath deposition (CBD) growth process, the aqueous solution of zinc nitrate hexahydrate [$Zn(NO_3)_2.6H_2O$], and hexamethylenetetramine ($C_6H_{12}N_4$) were first prepared. The concentrations of both were fixed at 0.1M. The aqueous solutions of zinc nitrate hexahydrate [$Zn(NO_3)_2.6H_2O$] (100 mL) and hexamethylenetetramine ($C_6H_{12}N_4$) (100 mL) were mixed together in 250 mL beaker. The bath is stirred at a constant rate of 360 RPM by magnetic stirrer for 30 minutes at room temperature. The beakers containing the bath solutions and the substrates were put on the hot plate for 2 h at a constant temperature of 93ºC. After the growth, the substrates were removed from the solutions, rinsed with acetone, distilled water, ethanol then acetone and dried at room temperature. A post growth annealing was performed for the substrates (samples) at 150ºC for 1 h and then quenched to room temperature (Li Z *et al*, 2008).

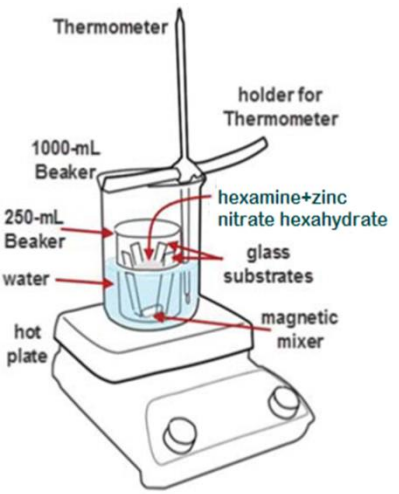

Figure 2: The schematic diagram of chemical bath depesotion of ZnO nanostructure

2.4 Characterization

Centrifuge machine (Kokusan H-200 series) was used to separate the colloid from the solutions. Silver nanoparticles and ZnO nanostructures such as nanoflowers and nanorods were confirmed X-ray powder diffractometer (XRD) (Type: RIGAKU–RINT 2000), and Scanning Electron Microscope (SEM) (Type: JEOL 15 kV).

Results and Discussions

3.1. UV and XRD Analysis of silver seed for CBD

Before fabricating the seeding layer, UV and XRD analysis are performed to determine the nature of Ag nanoparticles.

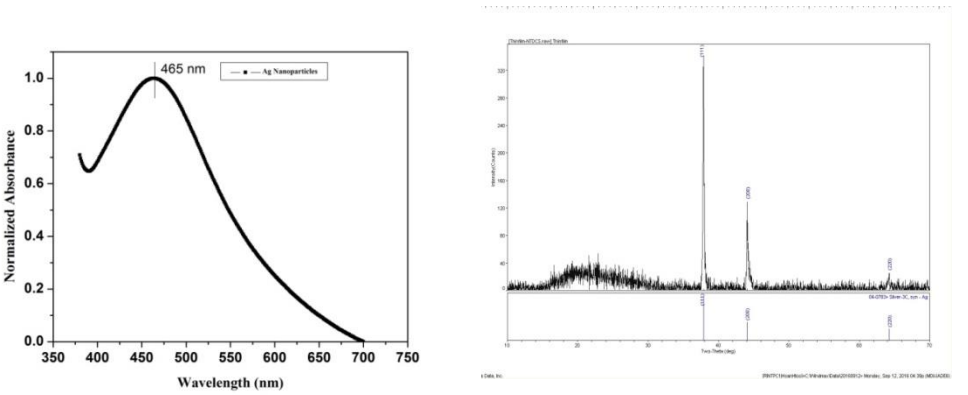

Figure 3 :(a) UV-Vis spectra of silver nanoparticle in which the absorptions at 465 nm were attributed to the plasmon resonance peaks of silver (b) XRD pattern of purified silver nanostructure

In Figure 3 (a) shows the uV-vis spectra of silver nanoparticles. The appearance of surface plasmon resonance (SPR) which can be attributed to the collective oscillation of conduction electrons that is induced by an electromagnetic field at 465 nm indicated the formation of AgNps. The symmetric shape of the SPR band indicates the formation of spherically shaped NPs, and the long tail in the red region indicates the formation of polydisperse size of NPs. The X-ray diffraction pattern of the silver nanowires synthesized by polyol method is shown in Figure 3 (b). A number of strong Bragg reflections can be seen which correspond to the (111), (200), and (311) reflections of FCC silver. No spurious diffractions due to crystallographic impurities are found, only monophase silver agrees with the XRD data (ICDD-PDF#04-0783). The high intense peak for FCC materials is generally (1 1 1) reflection, which is observed in the sample. The lattice constant calculated from the diffraction pattern was 0.4086 nm, which is in agreement with the reported value of silver (JCPDS 04-0783). From SEM data, SEM images show that spherical shaped silver nanoparticles have relatively uniform average diameter equal to 100 nm.

To compare ZnO nanostructures grown on different seed layers, SEM images of ZnO nanostructures on three types of Ag film were performed, as shown in Fig. 4, 5 and 6. The SEM characterizations of the seed layers and as-synthesized zinc oxide (ZnO) nanostructures are shown in Figure: 4, 5 and 6.

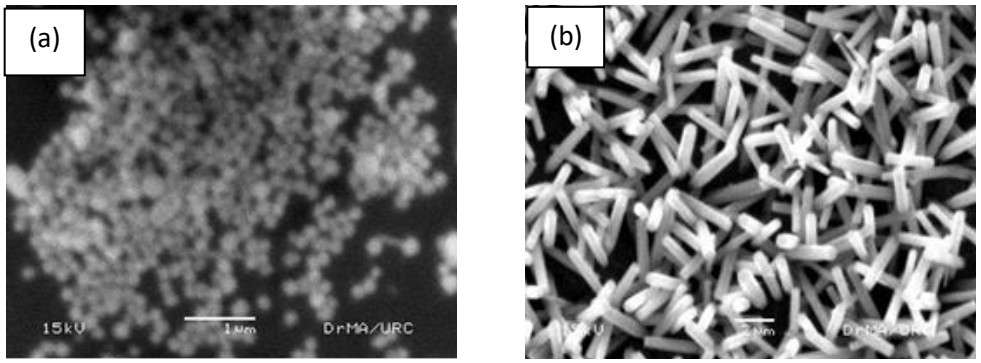

Figure 4:(a) Top-view SEM images of sample S1 (a) silver seed layer which is coated onetime on the glass substrate (b) ZnO nanorod which is grown on thin seed layer

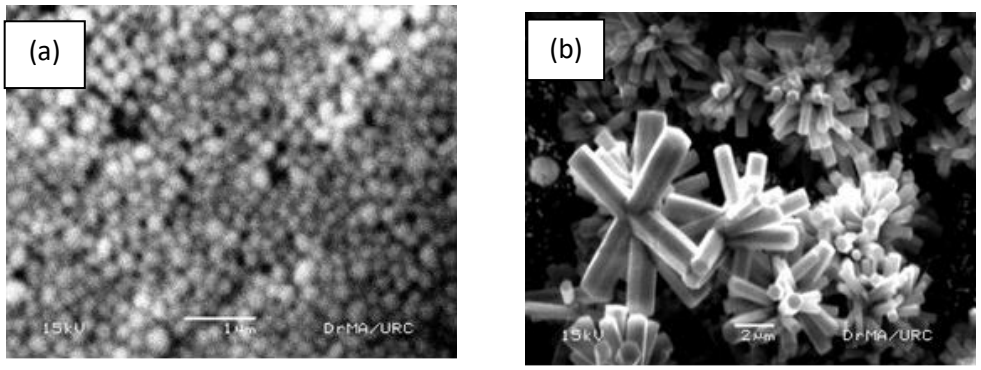

Figure 5: (a) Top-view SEM images of sample S1 (a) silver thickseed layer which is coated two times (b) ZnO nanorod which is grown on thicker seed layer

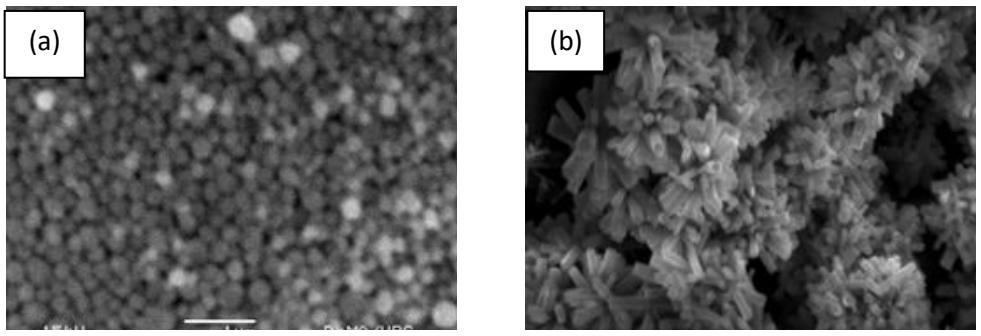

Figure 6: (a) Top-view SEM images of sample S3 (a) silver thick seed layer which is coated three times on the glass substrate(b) ZnO nanoflowers which is grown on thicker seed layer.

The SEM results revealed that the formation of nanorods and nanoflowers are formed in these samples. It is observed that the size of the nanorod and nanoflowers is depend on the seed layer. In Figure 3(b) SEM image shows that the length of the zinc oxide (ZnO) nanorods is 2μm in diameter from 200 nm to 300 nm. Figure 4(b) and 5(b) show that the lengths of zinc oxide (ZnO) nanoflowers were up to more than 2 μm and the diameter around 500 nm. It could be seen that the shape of ZnO nanoflowers resembled star-like morphology and the edges of ZnO petal were not smooth and were composed of assemblies of smaller nanocrystallites.

Ag seed films show symmetric and spherical NPs where the particles are uniformly distributed on the glass substrate. With increasing film thickness, more numbers of particles are deposited on top of each particle forming arrays of Ag NPs. The bottom Ag layer greatly influences the growth of ZnO nanostructure concerned to their aspect ratio, orientation, and density. With an increase in Ag seed layer film thickness, ZnO nanorods starts to grow in multiple directions leading to form flower like morphology could be called as nanoflower (i.e. growing more than 10 ZnO rods in a different direction ori- ginated from a single point) at thicker seed layer (Park WI *et al*, 2002).

The structural properties of the zinc oxide (ZnO) nanorods were characterized by X- ray diffraction (XRD). X-ray diffractomer, operated at 40kV and 40mA, with a Cu-Kα radiation (λ = 1.54056Å) in the range of 2θ between 10° and 70° as shown in Figure: 6. The upper site of (XRD) profile represented the observed XRD pattern while the lower site indicated the standard (reference) #PDF-76-0704 (Powder Diffraction File) Library file. The X-Ray Diffraction analysis shows that ZnO nanorod has a hexagonal crystallite structure with lattice parameters; a=b=3.2699 and c=5.2219 (a=b≠c), which agrees with the condition for a lattice structure to be hexagonal. The Debye-Scherrer's equation (equation 1) used to estimate the average crystallite size. The crystallite domain diameters *D* were obtained from XRD peaks according to the Debye-Scherrer's equation:

$$D=k\lambda/\beta\cos\theta \quad (1)$$

where, k is known as Scherrer's constant which is dependent on the crystallite shape and can be considered as 0.9, λ is the X-ray wavelength of the incident Cu Kα radiation, which is 0.154056 nm, β is the full width at half maximum of the respective peak and θ represents the diffraction peak angle. The calculated average crystallite size for zinc oxide (ZnO) nanoflower is 50 nm. The result showed that the (ZnO) nanorods that was prepared through the chemical bath deposition method presented a remarkably strong diffraction peak at the (002) plane, which is located between 34.23°. This finding indicated that of the (ZnO) nanoflower possessed hexagonal structure with high c-axis orientation. There is a significant increase in the intensity of the diffraction peak corresponding to the (002) plane perpendicular to the substrate. Meanwhile, the weak diffraction peaks of (100) and (101) also appear, as shown in the figure 4. The relative intensity ratio of *I(002)*, defined as *I(002) = I(002)/[I(100)+I(002)+I(101)]*, of the (ZnO) nanoflowers is 0.37. The XRD pattern exhibited that of the (ZnO) nanoflowers had remarkably excellent crystal quality and high c-axis orientation.

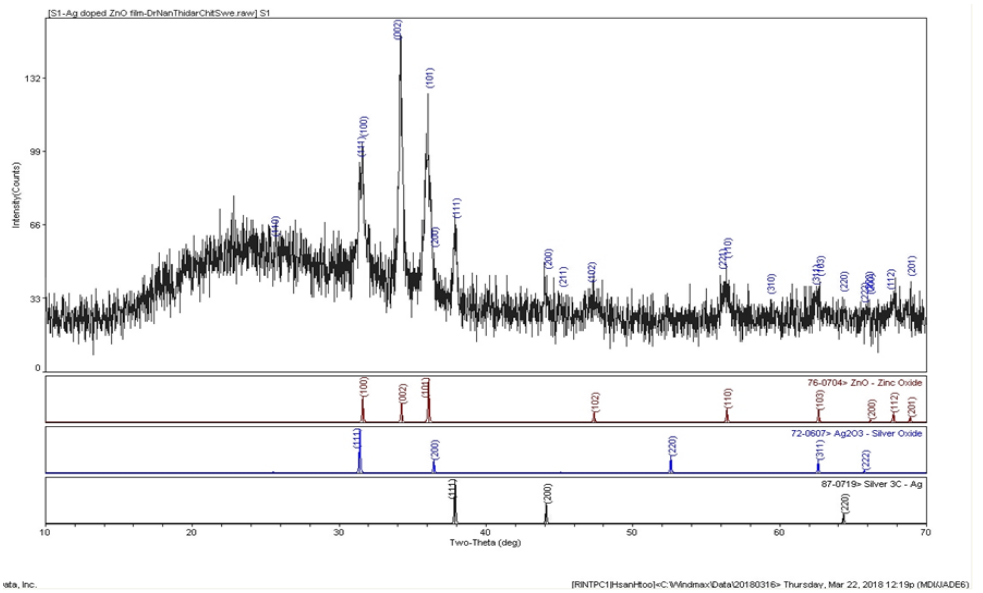

Figure 6: XRD plots obtained from ZnO nanostructures sample to investigate the structures and crystallinity. Reference bulk reflections of pure Ag and Ag2O3 phases are shown at the bottom (ICDD-PDF#07-0719), (ICDD-PDF#72-0607).

According to XRD result, ZnO nanostructures were heterogeneously grown on oxidized Ag layers. The ZnO nanostructure (lattice constant 1.5) are grown on a lattice-mismatched Ag/Ag_2O_3 (lattice constant 4.9) seed layer. These results explicit that ZnO nanorods can grow vertically on an oxidized Ag layer. Basically, the ZnO nucleation occurs at stable sites with lowest surface energy. The sites with large lattice mismatch between ZnO and metal substrate are forced to separate ZnO nucleus due to their high surface energy. To reduce surface energy and lattice mismatch, water molecules can oxidize the ionized metal layer using environmental thermal energy given by M++ OH- ,□ M(OH) ,□ $MO^- + H^+$, where M is metal. Usually, ionized metal atoms result from oxidized metal atoms, which have been exposed and oxidized in ambient air. These oxidation processes on metal surfaces are used to happen non-uniformly. In addition, the lattice constant of a metal oxide layer seriously affects the growth of ZnO nanostructures on itself. Therefore, when the both requirements are met, ZnO nanorod can be successfully grown on the metal oxide (Kashif M *et al*, 2012).

For the growth of the ZnO nanoflower following the growth of the nanorods, nucleation sites are formed on the surface of the ZnO nanorods with greater height because of the radial growth preference of the nanorods which is less spatially hindered. After the formation of the nucleation sites, many ZnO nanorods grow radially which finally results in the ZnO nanoflower structure (Karami H *et al*, 2011). Whereas non-uniformly localized metal oxide sites collect ZnO nucleus and grow ZnO nanowires along with the morphology of ZnO nucleus, Ag+ ions can oxidize metal surface very uniformly and metal atoms are negatively ionized easily to meet Zn2+ ions when Ag+ ions are detached (Lee GJ *et al*, 2010). Once ZnO islands are formed, ZnO nanoflowers are grown further on those islands following c-plane of ZnO.

Conclusion

Silver nanoparticles were synthesized by reducing $AgNO_3$ as metal precursor salt in Ethylene Glycol (EG) which was used as not only reducing agent but also solvent and PVP as a capping agent. In conclusion, zinc oxide (ZnO) nanoflowers were synthesized by a chemical bath deposition (CBD) method with wide range of size and various shapes. The petal lengths of the

zinc oxide (ZnO) nanoflowers were up to more than 2 μm and the diameter around 500 nm. It was observed that the length and alignment of (ZnO) nanoflowers were strongly related to the thickness of the seed layers.

Acknowledgements

The authors greatly indebted to Professor Dr Khin Khin Win, Head of Department of Physics, University of Yangon, for her kind permission to carry out this work. The authors wish to show our sincere thanks to Professor Dr Aye Aye Thant, Department of Physics, University of Yangon, for her fruitful discussions to this work. The authors acknowledge Professor Dr Ye Chan, Universities' Research Center, University of Yangon, for his advice and suggestions to this research and kind permissions to carry out laboratory facilities in URC.

References

Cao HL, Qian XF, Gong Q, Du WM, Ma XD, Zhu ZK: Shape- and size controlled synthesis of nanometre ZnO from a simple solution route at room temperature. Nanotechnology 2006, 17:3632.

D.H. Kim, H-J. Koo, J.S. Jur, M. Woodroof, B. Kalanyan, K. Lee, C.K. Devine, and G.N. Parsons, *Nanoscale*, 4 (2012) 4731-4738.

Feng L, Liu A, Ma Y, Liu M, Man B: Fabrication, structural characterization and optical properties of the flower-like ZnO nanowires. Acta Physiol Pol 2010, 117:512–517.

Gowthaman P, Saroja M, Venkatachalam M, Deenathayalan J, Senthil TS: Structural and optical properties of ZnO nanorods prepared by chemical bath deposition method. Aust J Basic Appl Sci 2011, 5:1379–1382.

Hossain M, Ghosh S, Boontongkong Y, Thanachayanont C, Dutta J: Growth of zinc oxide nanowires and nanobelts for gas sensing application. J Metastable Nanocrystalline Mater 2005, 23:27–30.

J. Liu, S. Xie, Y. Chen, X. Wang, H. Cheng, F. Liu, and J. Yang, *Nanoscale Res. Lett.*, 6 (2011) 619.

Karami H, Fakoori E: Synthesis and characterization of ZnO nanorods based on a new gel pyrolysis method. J Nanomater 2011, 2011:11.

Kashif M, Hashim U, Ali ME, Ali SMU, Rusop M, Ibupoto ZH, Willander M: Effect of different seed solutions on the morphology and electro optical properties of ZnO nanorods. J Nanomater 2012. 2012:6.

Li Z, Huang X, Liu J, Li Y, Li G: Morphology control and transition of ZnO nanorod arrays by a simple hydrothermal method. Mater Lett 2008, 62:1503–1506

L-W. Ji, S-M. Peng, J-S. Wu, W-S. Shih, C-Z. Wu, and I-T. Tang, *J. Phys. Chem. Solids*, 70 (2009) 1359.

Lee GJ, Lee Y, Lim HH, Cha M, Kim SS, Cheong H, Min SK, Han S,H: Photoluminescence and lasing properties of ZnO nanorods. J Korean Phys Soc 2010, 57:1624–1629.

Nan TD, Lwin KO, Thida M, Ye C: Polyol Synthesis of Silver Nanoparticles for Flexible Electronic Circuit. Universities Research Journal, 2018, Vol.11.

Park WI, Kim DH, Jung S-W, Yi G-C: Metalorganic vapor-phase epitaxial growth of vertically well-aligned ZnO nanorods. Appl Phys Lett 2002,80:4232–4234.

Samanta P, Patra S, Chaudhuri P: Visible emission from ZnO nanorods synthesized by a simple wet chemical method. Int J Nanosci Nanotech 2009, 1:81–90.

Xia Y, Yang P, Sun Y, Wu Y, Mayers B, Gates B, Yin Y, Kim F, Yan H: One dimensional nanostructures: synthesis, characterization, and applications. Adv Mater 2003, 15:353–389.

Yi S-H, Choi S-K, Jang J-M, Kim J-A, Jung W-G: Low-temperature growth of ZnO nanorods by chemical bath deposition. J Colloid Interface Sci 2007, 313:705–710.